Overcoming the Out-of-Plane Bending Issue in an Aromatic Hydrocarbon: The Anharmonic Vibrational Frequencies of *c*-(CH)C$_3$H$_2^+$

SCHOLARONE™
Manuscripts

Journal Name

Overcoming the Out-of-Plane Bending Issue in an Aromatic Hydrocarbon: The Anharmonic Vibrational Frequencies of c-(CH)C$_3$H$_2^{+\dagger}$

Brent R. Westbrook[a], Weston A. Del Rio[a], Timothy J. Lee[b], and Ryan C. Fortenberry[a]

The challenges associated with the out-of-plane bending problem in multiply-bonded hydrocarbon molecules can be mitigated in quartic force field analyses by varying the step size in the out-of-plane coordinates. Carbon is a highly prevalent element in astronomical and terrestrial environments, but this major piece of its spectra has eluded theoretical examinations for decades. Earlier explanations for this problem focused on method and basis set issues, while this work seeks to corroborate the recent diagnosis as a numerical instability problem related to the generation of the potential energy surface. Explicit anharmonic frequencies for c-(CH)C$_3$H$_2^+$ are computed using a quartic force field and the CCSD(T)-F12b method with cc-pVDZ-F12, cc-pVTZ-F12, and aug-cc-pVTZ basis sets. The first of these is shown to offer accuracy comparable to that of the latter two with a substantial reduction in computational time. Additionally, c-(CH)C$_3$H$_2^+$ is shown to have two fundamental frequencies at the onset of the interstellar unidentified infrared bands, at 5.134 and 6.088 μm or 1947.9 and 1642.6 cm^{-1}, respectively. This suggests that the results in the present study should assist in the attribution of parts of these aromatic bands, as well as provide data in support of the laboratory or astronomical detection of c-(CH)C$_3$H$_2^+$.

1 Introduction

As the fourth most abundant element in the universe and a molecular building block for our current understanding of life, carbon plays a large role in the chemistry of interstellar molecules.[1–3] Despite this ubiquity, recently there has been significant difficulty in determining the anharmonic out-of-plane bending (OPB) frequencies of multiply-bonded hydrocarbons,[4–6] even using the best electronic structure methods. Over the last ~30 years, similar failings have been observed in the harmonic frequencies of ethylene,[7,8] acetylene,[9–11] benzene and other arenes,[12–14] as well as in nucleobases[15] but only when using wavefunction-based electron correlation methods. In other words, this issue with harmonic frequencies for small molecules having C=C multiple bonds, including aromatic systems, is not found at the Hartree-Fock (HF) or Density Functional Theory (DFT) levels of theory. In these cases, the harmonic frequencies can be so poorly described that the equilibrium structures of the molecules actually become bent.

However, there are also recent reports where the harmonic frequencies of large polycyclic aromatic hydrocarbon (PAH) molecules exhibit problems with harmonic frequencies,[16,17] again to the extent that the molecules are no longer planar and become bent. In these cases, though, the problem occurs using DFT methods that do not exhibit this problem for small PAH molecules. One question then arises, are these three different issues, 1) DFT harmonics, 2) wavefunction harmonics, and 3) wavefunction anharmonics, part of the same problem, or are they unrelated?

The problem with anharmonic OPB vibrational frequencies has been explored for the simple example of c-C$_3$H$_2$, cyclopropenylidene,[4–6] although previous studies have not found a problem.[18,19] Two of these studies examined the possibility that the OPB harmonic and anharmonic frequency issues when using wavefunction-based electron correlation methods, such as coupled cluster theory at the singles, doubles, and perturbative triples level [CCSD(T)],[20] are related and may be both a method and basis set issue, or in other words, due to a coupling of the one and n-particle effects.[4,5] In these studies, a quartic force field (QFF) was determined using the CCSD(T) method, and vibrational second order perturbation theory (VPT2) was used to determine the anharmonic vibrational frequencies.

a Department of Chemistry & Biochemistry, University of Mississippi, University, MS 38677-1848, USA. E-mail: r410@olemiss.edu
b MS 245-3, NASA Ames Research Center, Moffett Field, CA 94035, USA.

QFFs are fourth-order Taylor series expansions of the internuclear Watson Hamiltonian[21] utilized to compute anharmonic vibrational frequencies. At a high level the energies used to define the QFF are composites of complete basis set (CBS) extrapolations, core electron correlation, and scalar relativity, leading to the "CcCR" moniker. However, even this CcCR QFF, which frequently achieves accuracy within 1.0 cm^{-1} of gas-phase experiment,[22–32] falls short of both previous computational work[19] and argon-matrix experiment[33] in describing certain fundamental vibrational frequencies, notably the OPBs. As a result, further exploration[5] sought alternative paths to more accurate theoretical results via explicit correlation and various scaling factors for force constants. Although a hybrid QFF composed of the CcCR and explicitly-correlated results produced data in reasonable agreement with experiment, the authors acknowledge that this scheme is not reliably extensible to other molecules.[5]

However, in a later study, it was determined that the OPB anharmonic frequencies for c-C_3H_2 come into line when the displacements used for the OPB symmetry internal coordinates to determine the QFF are increased, suggesting that there were not enough significant digits in the OPB energies.[34] Symmetry internal coordinates are a key portion of the QFF methodology, as they define the numerical derivatives taken to map the potential energy surface. The typical step length is 0.005 Å in the internuclear distances and 0.005 radians in the bending and torsional coordinates. This has previously been shown to be the optimal size[22,23] for general applications, but the step size has proven to be a tunable variable that can improve (or degrade) results for certain applications. This is especially true when the energy differences in question are small, which jeopardizes the numerical stability of the QFF as a whole.[34] Taking larger steps can induce more significant energy differences, which allows for computation of the numerical derivatives without substantial loss of precision. Even so, care must be taken when doing so as higher-order contamination in the force constants, especially the quartic constants, can also be introduced with larger step sizes. Hence, there is a balance. As such, one of the goals of the present work is to explore further the effects of step size on the treatment of the OPB problem.

The specific interest in c-(CH)$C_3H_2^+$, the molecule of the present study, is two-fold. First, the structure is similar to that of cyclopropenylidene, which has been well-studied in its exhibition of the out-of-plane bending problem. Second, c-(CH)$C_3H_2^+$ is also closely related to the cyclopropenylidenyl carbene (c-(C)C_3H_2), which has previously been shown to have fundamental vibrational frequencies in the mid-IR, within the range of the unidentified infrared bands (UIRs).[35–39] These interstellar spectral bands stretch from the near- to far-IR and have thus far been largely unattributed.[37,38] As such, the vibrational and rotational spectroscopic data reported herein will not only allow for the identification and characterization of c-(CH)$C_3H_2^+$ in both the laboratory and in regions of astrochemical interest, but it may also serve to help disentangle the some spectral features of the UIRs. The fundamental frequencies in the infrared range will pair well with the infrared focus of the upcoming *James Webb Space Telescope* (*JWST*) and with the currently operating *Stratospheric Observatory for Infrared Astronomy* (*SOFIA*) as they examine the heavens

in these wavelengths.

The other major focus of the current work is to examine the difference in accuracy between using double- and triple-ζ basis sets[11,40,41] designed to work with the CCSD(T)-F12 method and a typical Dunning triple-ζ basis set augmented with diffuse functions.[42,43] The first of these (cc-pVDZ-F12) obviously will lead to faster computations allowing for the analysis of much larger hydrocarbon molecules, possibly even small PAHs. However, the latter two presumably will offer greater accuracy, but it remains to be tested whether or not this improvement is sufficient to justify the greater computational cost as has been demonstrated in some molecular systems.[44] If triple-ζ quality is required to adequately treat these systems, there further remains the choice between the F12 and augmented basis sets. Previous QFF studies[4,5,35,44,45] have variously made use of both types, but further data is needed in order to clarify the advantages of each.

2　Computational Details

Geometry optimizations and harmonic frequency computations are performed using the Molpro 2015.1 software package[46] at the coupled cluster singles, doubles, and perturbative triples level of theory[20] within the F12 explicitly correlated construction (CCSD(T)-F12b).[47,48] The cc-pVDZ-F12[40] basis set is used for the initial survey of potential step sizes, while both the cc-pVTZ-F12[11,40,41] and the aug-cc-pVTZ[42,43] basis sets are used for the final, "best guess" step size computations. These schemes are abbreviated as F12-DZ, F12-TZ, and F12-aTZ in the following. The dipole moment computation is done at the F12-TZ level. Double-harmonic intensity calculations utilize the Gaussian16 program at the MP2/6-31+G(d) level of theory,[49,50] with this scheme previously shown to give semi-quantitative agreement with more computationally-demanding levels of theory.[51,52]
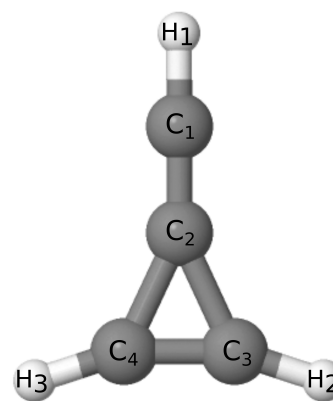
Fig. 1 Visual depiction of the c-(CH)$C_3H_2^+$ molecule

Explicit anharmonic vibrational frequencies are computed using a QFF approach at these aforementioned levels of theory. The QFF methodology utilized herein requires the optimization of the molecular geometry to give the reference configuration, followed by 10353 single-point energy computations for displacements of the symmetry-internal coordinates. In the F12-DZ computations, these displacements are varied from 0.005 to 0.040 radians for coordinates 14 and 15 but kept constant at 0.005 Å or radians

for the other bond lengths and angles/torsions, respectively. Both sets of the TZ computations use displacements of 0.020 Å/radians for coordinates 14 and 15. The symmetry-internal coordinates, with atom labels given in Figure 1 are as follows:

$$S_1(a_1) = r(H_1 - C_1) \quad (1)$$

$$S_2(a_1) = r(H_1 - C_2) \quad (2)$$

$$S_3(a_1) = \frac{1}{\sqrt{2}}[r(C_2 - C_3) + r(C_2 - C_4)] \quad (3)$$

$$S_4(a_1) = \frac{1}{\sqrt{2}}[r(C_3 - H_2) + r(C_4 - H_3)] \quad (4)$$

$$S_5(a_1) = \frac{1}{\sqrt{2}}[\angle(C_1 - C_2 - C_3) + \angle(C_1 - C_2 - C_4)] \quad (5)$$

$$S_6(a_1) = \frac{1}{\sqrt{2}}[\angle(C_2 - C_3 - H_2) + \angle(C_2 - C_4 - H_3)] \quad (6)$$

$$S_7(b_2) = \frac{1}{\sqrt{2}}[r(C_2 - C_3) - r(C_2 - C_4)] \quad (7)$$

$$S_8(b_2) = \frac{1}{\sqrt{2}}[r(C_3 - H_2) - r(C_4 - H_3)] \quad (8)$$

$$S_9(b_2) = \frac{1}{\sqrt{2}}[\angle(C_1 - C_2 - C_3) - \angle(C_1 - C_2 - C_4)] \quad (9)$$

$$S_{10}(b_2) = \frac{1}{\sqrt{2}}[\angle(C_2 - C_3 - H_2) - \angle(C_2 - C_4 - H_3)] \quad (10)$$

$$S_{11}(b_2) = \frac{1}{\sqrt{2}}[\angle(H_1 - C_2 - C_3) - \angle(H_1 - C_2 - C_4)] \quad (11)$$

$$S_{12}(b_1) = OPB(H_1 - C_2 - C_3 - C_4) \quad (12)$$

$$S_{13}(b_1) = OPB(C_1 - C_2 - C_3 - C_4) \quad (13)$$

$$S_{14}(b_1) = \frac{1}{\sqrt{2}}[\tau(C_1 - C_2 - C_3 - H_2) - \tau(C_1 - C_2 - C_4 - H_3)] \quad (14)$$

$$S_{15}(a_2) = \frac{1}{\sqrt{2}}[\tau(C_1 - C_2 - C_3 - H_2) + \tau(C_1 - C_2 - C_4 - H_3)], \quad (15)$$

with "OPB" referring, again, to an out-of-plane bending motion.

Following the single-point computations, the QFF function is fit by a least-squares method, yielding sums of squared residuals on the order of 10^{-14} a.u.^{2} or less in all cases. The resulting fitted function produces a new equilibrium geometry and the corresponding refitting zeroes the gradients and generates the final force constants. These force constants are transformed by the INTDER[53] program into Cartesian coordinates for use in second-order rotational[54] and vibrational perturbation theory (VPT2)[55,56] via the SPECTRO[57] program. The force constants produced by each level of theory are given in the Supplemental Information. Fermi and Coriolis resonances are further included to increase the accuracy of the anharmonic results.[58,59] c-(CH)C$_3$H$_2^+$ has nine type 1 Fermi resonances, 13 type 2 Fermi resonances, and five Coriolis resonances, of which one is A type,

three are B type, and one is C type. These resonances are also given in the Supplemental Information.

3 Results and Discussion

Table 1 Harmonic and anharmonic frequencies (in cm^{-1}) for c-(CH)C$_3$H$_2^+$ at various step sizes (in Å/rad)

Mode	Description	Symmetry	0.0050	0.0075	0.0100	0.0200	0.0400
ω_1	$0.96S_1$	a_1	3371.6	3371.5	3371.5	3371.5	3371.5
ω_2	$0.95S_4$	a_1	3328.3	3328.3	3328.3	3328.3	3328.3
ω_3	$1.00S_8$	b_2	3262.9	3262.9	3262.9	3262.9	3262.9
ω_4	$0.68S_2 + 0.28S_3$	a_1	1975.7	1975.7	1975.7	1975.7	1975.7
ω_5	$0.74S_5 + 0.24S_2$	a_1	1681.5	1681.5	1681.5	1681.5	1681.5
ω_6	$0.90S_{10} + 0.12S_9$	b_2	984.9	984.9	984.9	984.9	984.9
ω_7	$0.58S_{11} + 0.31S_9 + 0.09S_{10}$	b_2	915.8	915.8	915.8	915.8	915.8
ω_8	$1.03S_6$	a_1	910.4	910.4	910.4	910.4	910.4
ω_9	$0.71S_3 + 0.27S_5 + 0.04S_2$	a_1	764.7	764.7	764.7	764.7	764.7
ω_{10}	$1.00S_{15}$	a_2	718.5	718.3	718.2	718.1	718.0
ω_{11}	$1.26S_{14} - 0.29S_{13}$	b_1	715.3	715.0	714.9	714.8	714.8
ω_{12}	$1.04S_7 - 0.05S_9$	b_2	571.4	571.4	571.4	571.4	571.4
ω_{13}	$0.98S_{12}$	b_1	497.7	497.7	497.7	497.7	497.7
ω_{14}	$1.28S_{13} - 0.28S_{14}$	b_1	351.6	351.1	350.9	350.7	350.7
ω_{15}	$0.62S_9 + 0.42S_{11} - 0.06S_7$	b_2	144.8	144.8	144.8	144.8	144.8
ZPVE			10052.0	9966.7	9949.2	9941.6	9983.4
ν_1		a_1	3242.3	3238.6	3238.2	3238.1	3243.2
ν_2		a_1	3185.0	3184.0	3183.6	3183.6	3188.7
ν_3		b_2	3132.8	3131.4	3130.9	3130.7	3134.4
ν_4		a_1	1949.0	1946.8	1946.6	1947.9	1951.5
ν_5		a_1	1643.1	1641.8	1641.8	1642.6	1644.0
ν_6		b_2	974.7	974.2	971.9	971.0	986.2
ν_7		b_2	920.1	887.7	886.8	917.3	923.1
ν_8		a_1	901.2	894.3	895.3	894.5	913.4
ν_9		a_1	766.1	716.7	707.1	757.2	760.5
ν_{10}		a_2	723.4	706.0	701.4	697.8	698.7
ν_{11}		b_1	801.3	722.0	706.9	698.1	698.0
ν_{12}		b_2	542.6	540.7	540.2	539.8	543.4
ν_{13}		b_1	488.5	490.6	490.7	491.0	493.8
ν_{14}		b_1	378.3	201.1	162.6	137.2	138.4
ν_{15}		b_2	235.0	209.0	203.5	201.5	300.5

3.1 Effects of step size

As shown in Table 1, changing the size of the steps in coordinates 14 and 15 has virtually no effect on the harmonic frequencies, even those in which these coordinates make the dominant contribution, in line with expected behavior for more advanced quantum chemical theories like CCSD(T)-F12.[5] However, the zero-point vibrational energy (ZPVE) and the anharmonic frequencies are clearly more substantially affected. Starting from the first fundamental row of Table 1, even ν_1, which is composed nearly entirely of coordinate S_1 varies by nearly 5.0 cm^{-1} as a result of the step size change to coordinates 14 and 15 and the subsequent refitting for each new QFF. This is within the expected accuracy of this QFF methodology but is indicative of the potentially great influence of step size on the resulting frequencies after the anharmonic fitting is included. The greatest disparities between the various data occur in ν_{11}, ν_{14}, and ν_{15}, with the largest difference among these constituting 100 cm^{-1}. Despite the disagreement between the values reported for the different step sizes in these modes, ν_{11} and ν_{14} show convergence as the step size increases, suggesting that some of the problematic nature of these modes is mitigated by larger step sizes. ν_{15}, somewhat similarly, appears to converge as the step size increases from 0.005 to 0.020, but at the largest step size it increases substantially.

The lowering of ν_{15} with increasing step size is due to the less hindered motion of the C$_1$ atom (from Figure 1) in the plane of the molecule at larger step sizes. ν_{15} is composed of the in-plane motion of H$_1$ and C$_1$, which is resisted by the presence of H$_2$ and H$_3$ at small step sizes. Increasing the amount by which these terminal hydrogens are shifted out of the plane leaves more room for the in-plane bending motion of the apical carbon and hydrogen,

lowering the associated energy of that motion and consequently lowering the frequency. This is consistent with the initial lowering of this fundamental from a step size of 0.005 to 0.020, but the final increase in the frequency at the greatest step size requires a different explanation. A similar trend has been observed previously at larger step sizes, and is the result of contamination by higher-order effects.[23] As such, the optimal step size must balance these two sources of instability.

Table 2 Harmonic and anharmonic force constants (in mdyn Å^{-n}) for c-$(CH)C_3H_2^+$ at various step sizes (in Å/rad)

Force Constant	Step Size				
	0.0050	0.0075	0.0100	0.0200	0.0400
$F_{13,13}$	2.459597	2.459591	2.459591	2.459592	2.459595
$F_{13,14}$	-0.563628	-0.563628	-0.563628	-0.563628	-0.563627
$F_{14,14}$	0.165021	0.164944	0.164917	0.164890	0.164883
$F_{15,15}$	0.122144	0.122048	0.122015	0.121982	0.121972
$F_{13,13,13,13}$	1735.47	1469.46	1469.46	1469.46	1469.48
$F_{13,13,13,14}$	-25.29	-27.01	-27.01	-27.01	-27.01
$F_{13,13,14,14}$	2.63	2.61	2.53	2.46	2.44
$F_{13,14,14,14}$	0.01	0.01	0.01	0.01	0.01
$F_{14,14,14,14}$	0.24	0.05	0.01	0.00	0.00
$F_{15,15,15,15}$	0.42	0.21	0.18	0.16	0.17

While the harmonic frequencies are generally unchanged, there are still some notable differences for ω_{10}, ω_{11}, and ω_{14}, where the greatest differences in the anharmonic frequencies are also observed. ω_{10} is solely comprised of coordinate S_{15}, while ω_{11} and ω_{14} are combinations of S_{13} and S_{14}. All three of these coordinates correspond to the OPB motions for the substituents on the cyclopropenyl ring. The changes in the associated force constants are in line with these changes in the frequencies, as shown in Table 2.

The associated harmonic force constants differ on the order of 10^{-4} mdyn Å^{-2} between all of the step sizes, and correspondingly, the precision reported in Table 2 shows no difference between them in almost every case. The remaining differences do lead to nearly 1.0 cm^{-1} of variation in ω_{14}, but this is well within the expected accuracy of the method. This is further in agreement with previous work, which showed that problems in the harmonic frequencies could be reduced by using more advanced quantum chemical methods, such as those used herein.[4–6] Similarly, the disagreement of the anharmonic force constants is indicative of the expected lingering deficiency in the anharmonic treatment of these modes. The effect of step size is most clearly apparent in $F_{13,13,13,13}$, which decreases by nearly 300 mdyn Å^{-4} when moving from a step size of 0.005 to 0.0075, representing a change of more than 15%. Again, the changed step sizes are only in coordinates S_{14} and S_{15}, so the effects of these changes extend beyond the force constants associated directly with these coordinates and affect other quartic force constants through coupling, as well as alter the QFF fitting itself.

The differences in the rest of the anharmonic force constants are much smaller, with that of $F_{13,13,13,14}$ being the next largest at 1.8 mdyn Å^{-4} or about 7%. As also observed in the anharmonic frequencies of Table 1, the force constants appear to be converging as the step size increases from 0.005 to 0.020, even in the case of $F_{13,13,13,13}$, which is mostly converged as soon as the step size is increased beyond 0.005. There is again slightly more variance in the behavior at the extreme 0.040 step size, but none of the force constants at this step size behave particularly suspiciously.

Further, the magnitude of the force constants below $F_{13,13,14,14}$ is so small that any differences will have only a small effect on the frequencies as well.

Overall, the apparently convergent effect of the varied step sizes from 0.005 to 0.020 on both the force constants and the frequencies suggests that 0.020 is the optimal step size for coordinates 14 and 15 in this system. The fact that a step of 0.010 leads to the minimum in some cases indicates that it may be hitting this sweet spot, too, but 0.020 better handles all modes more frequently presently in the case of c-$(CH)C_3H_2^+$. Consequently, this is the step size utilized in the more computationally demanding F12-TZ and F12-aTZ computations.

3.2 Level of theory

Table 3 Harmonic and anharmonic frequencies (in cm^{-1}) for c-$(CH)C_3H_2$ with various basis sets

Mode	Symmetry	DZ/F12	TZ/F12	TZ/aVTZ	f
ω_1	a_1	3371.5	3370.7	3370.2	121
ω_2	a_1	3328.3	3326.3	3325.9	76
ω_3	b_2	3262.9	3261.1	3260.5	234
ω_4	a_1	1975.7	1975.9	1977.3	186
ω_5	a_1	1681.5	1681.1	1681.3	67
ω_6	b_2	984.9	985.9	985.5	8
ω_7	b_2	915.8	919.2	920.6	3
ω_8	a_1	910.4	909.0	908.2	7
ω_9	a_1	764.7	767.6	768.6	63
ω_{10}	a_2	718.1	718.7	713.1	0
ω_{11}	b_1	714.8	715.5	711.5	77
ω_{12}	b_2	571.4	577.5	580.4	22
ω_{13}	b_1	497.7	502.0	509.3	112
ω_{14}	b_1	350.7	356.2	355.9	0
ω_{15}	b_2	144.8	149.8	155.7	46
ZPVE		9941.6	9971.0	9954.2	
ν_1	a_1	3238.1	3238.7	3237.1	
ν_2	a_1	3183.6	3184.9	3182.2	
ν_3	b_2	3130.7	3131.9	3130.1	
ν_4	a_1	1947.9	1948.0	1947.8	
ν_5	a_1	1642.6	1642.3	1641.9	
ν_6	b_2	971.0	974.4	970.1	
ν_7	b_2	917.3	890.4	894.0	
ν_8	a_1	894.5	902.3	884.4	
ν_9	a_1	757.2	725.4	760.2	
ν_{10}	a_2	697.8	703.6	713.0	
ν_{11}	b_1	698.1	702.0	729.0	
ν_{12}	b_2	539.8	546.0	547.4	
ν_{13}	b_1	491.0	490.7	480.8	
ν_{14}	b_1	137.2	160.6	154.3	
ν_{15}	b_2	201.5	248.1	175.9	

As alluded to previously, both cc-pVXZ-F12 basis sets designed for use with CCSD(T)-F12 methods and general-purpose aug-cc-pVXZ sets have been used in the generation of QFFs in the literature.[4,5,35,44,45] One goal of the present study then is to elucidate the effects of these different bases. Another aim is determining whether the accuracy gains in using either triple-ζ basis set are worth the greater computational demand, at least for the generation of QFFs on similar molecules. As shown in Table 3, the effects

of the various basis sets are generally minimal. The differences in the harmonic frequencies are greater than those resulting from changing the step size, but the fundamental frequencies are more similar overall. In particular, the well-described, high-frequency fundamentals are nearly identical across the treatments, with the greatest disparity occurring in v_2 of only 2.6 cm^{-1}, well within the expected 5-7 cm^{-1} accuracy of an F12-TZ QFF.

From about 750 cm^{-1} and down, the agreement between the treatments begins to break down somewhat, and there is no clear trend between them. Consequently, in lieu of comparable experimental data, determining which is the most accurate is largely impossible. However, the F12-TZ and F12-aTZ single-point energy computations required 6600814 seconds (76.4 days) and 5768556 seconds (66.8 days) of wall time to run, respectively, while the corresponding F12-DZ points needed only 845395 seconds (9.8 days). While these absolute times are obviously reduced by running in parallel, this still represents nearly an order of magnitude of difference in the computational requirements. Thus, for at least the prediction of the high frequency fundamentals, the much less expensive DZ computations seem acceptably accurate and they may fortuitously capture accurate frequencies for the lower frequency modes as well.

3.3 Spectroscopic considerations

The intensities reported in Table 3 indicate that nearly every vibrational frequency will be visible to vibrational spectroscopy, with the clear exceptions of v_{10} and v_{14}. v_6, v_7, and v_8 also have very small intensities, which may make them difficult to pinpoint, but v_3 and v_4, for example, have intensities several-fold greater than the antisymmetric stretch in water, making these good targets for spectroscopic investigation. As mentioned above, there is no clear accuracy advantage for any of the results presented in Table 3, so any or all of them may be necessary to help identify this molecule in the laboratory and in astronomical environments.

With regard to the rotational data, the same standards apply. The accuracy of the three levels of theory examined herein should be roughly comparable, at least without experimental validation of a particular data set. Previous work has shown that the accuracy of the rotational constants is not as high as that of the vibrational data, but it should still be accurate to within 30 MHz for the B and C rotational constants.[22–24,26,27,29,30,32,60–68] The absolute agreement for the A constants is typically less impressive, but this often has to do with the greater relative magnitude of this constant in near-prolate molecules. Regardless, c-(CH)C$_3$H$_2^+$ is near-prolate, with its A constant being much greater than the B and C constants, which are of the same magnitude. This relationship is evident in Table 4. Additionally, its small but non-zero dipole moment of 0.2 D could allow for its observation by rotational spectroscopy in conjunction with examination via vibrational spectroscopy.

4 Conclusions

The results of this study and that of Ref. 34 suggest that the three different issues discussed in the introduction for OPB vibrational frequencies of C=C multiply-bonded systems may be

Table 4 Geometrical parameters and rotational constants for c-(CH)C$_3$H$_2$

	DZ/F12	TZ/F12	TZ/aVTZ
R(H1-C1) (Å)	1.07249	1.07237	1.07257
R(C1-C2) (Å)	1.23336	1.23286	1.23324
R(C2-C3/4) (Å)	1.51874	1.51723	1.51734
R(C3/4-H2/3) (Å)	1.07777	1.07776	1.07791
R(C3-C4) (Å)	1.27078	1.27039	1.27077
∠(C2-C3/4-H2/3) (Deg)	132.722	132.701	132.718
A_0 (MHz)	32944.4	32962.1	32950.4
B_0 (MHz)	7438.9	7449.9	7446.2
C_0 (MHz)	6055.4	6063.5	6060.9
A_1 (MHz)	32941.3	32959.2	32947.4
B_1 (MHz)	7422.3	7433.3	7429.6
C_1 (MHz)	6044.6	6052.5	6049.9
A_2 (MHz)	32764.8	32783.4	32771.9
B_2 (MHz)	7437.5	7448.6	7444.8
C_2 (MHz)	6048.5	6056.7	6054.0
A_3 (MHz)	32785.2	32803.7	32792.3
B_3 (MHz)	7436.2	7447.3	7443.5
C_3 (MHz)	6048.4	6056.5	6053.9
A_4 (MHz)	32880.9	32898.0	32886.9
B_4 (MHz)	7416.5	7427.7	7423.9
C_4 (MHz)	6038.3	6046.4	6043.8
A_5 (MHz)	32769.2	32788.2	32775.8
B_5 (MHz)	7449.4	7460.3	7456.6
C_5 (MHz)	6056.9	6065.0	6062.4
A_6 (MHz)	33100.6	33122.4	33108.7
B_6 (MHz)	7452.1	7462.8	7458.8
C_6 (MHz)	6051.5	6059.6	6057.0
A_7 (MHz)	33290.0	33305.7	33296.3
B_7 (MHz)	7436.8	7452.2	7448.3
C_7 (MHz)	6051.1	6059.3	6056.6
A_8 (MHz)	33035.8	33054.4	33042.8
B_8 (MHz)	7436.0	7447.1	7443.3
C_8 (MHz)	6052.4	6060.6	6058.0
A_9 (MHz)	32938.2	32956.0	32943.0
B_9 (MHz)	7416.5	7427.4	7423.6
C_9 (MHz)	6032.4	6040.4	6037.9
A_{10} (MHz)	32887.0	32903.7	32890.2
B_{10} (MHz)	7414.7	7422.0	7443.2
C_{10} (MHz)	6053.5	6061.6	6065.3
A_{11} (MHz)	32882.7	32900.5	32895.4
B_{11} (MHz)	7435.5	7446.6	7418.7
C_{11} (MHz)	6059.8	6067.8	6059.0
A_{12} (MHz)	33213.6	33228.6	33220.8
B_{12} (MHz)	7380.9	7392.1	7389.0
C_{12} (MHz)	6007.8	6016.1	6013.9
A_{13} (MHz)	32596.8	32610.1	32585.3
B_{13} (MHz)	7455.7	7466.7	7462.1
C_{13} (MHz)	6071.4	6079.5	6076.2
A_{14} (MHz)	33329.2	33351.7	33357.6
B_{14} (MHz)	7453.0	7463.2	7459.7
C_{14} (MHz)	6073.4	6081.0	6078.6
A_{15} (MHz)	32345.2	32372.6	32356.0
B_{15} (MHz)	7507.0	7516.4	7509.9
C_{15} (MHz)	6078.9	6086.4	6082.7
Δ_J (kHz)	1.995	1.988	1.982
Δ_K (kHz)	-77.044	-71.533	-64.557
Δ_{JK} (kHz)	132.904	127.446	120.461
δ_J (kHz)	0.391	0.391	0.389
δ_K (kHz)	71.541	68.800	65.292
Φ_J (μHz)	-146.584	-146.294	-138.891
Φ_K (Hz)	32.684	28.851	24.618
Φ_{JK} (Hz)	5.034	4.542	3.950
Φ_{KJ} (Hz)	-37.613	-33.288	-28.463
ϕ_j (μHz)	58.733	57.774	59.440
ϕ_{jk} (Hz)	2.515	2.269	1.973
ϕ_k (Hz)	29.864	27.081	23.855

unrelated and separate issues, but this will require further study. Regardless, this work has demonstrated that increasing the QFF step size can improve the treatment of OPB anharmonic frequencies for these systems, in line with previous findings.[34] In this case, 0.020 Å/rad likely offers the most trustworthy step size, but 0.010 may perform better on other systems. Further, the performance of explicitly-correlated coupled cluster methods in conjunction with a double-ζ basis set is shown to be roughly equal to that of the same method with the comparable triple-ζ basis while demonstrating a significant reduction in the computational requirements.

The most accurate vibrational and rotational data for c-(CH)C$_3$H$_2^+$ available is provided to aid in its detection and characterization in the laboratory and in regions of astronomical interest. The addition of a proton blue-shifts the carbon-carbon double bond stretching modes relative to those of c-(C)C$_3$H$_2$[35] and places these frequencies at the onset of the carbon-carbon stretching modes typically attributed to PAHs in the UIRs.[36] Namely, v_4 and v_5 correspond to frequencies of 5.134 and 6.088 μm, respec-

tively. As such, the present data may help to disentangle some of the spectroscopic features observed by *SOFIA* and the upcoming *James Webb Space Telescope*. The methodology used herein will further help to elucidate spectra for larger PAH molecules, of which this molecule is a minimal example.

Conflicts of interest

There are no conflicts to declare.

Acknowledgements

Notes and references

1 B. D. Savage and K. R. Sembach, *Annu. Rev. Astron. Astrophys.*, 1996, **34**, 279–329.

2 J. A. Cardelli, D. M. Meyer, M. Jura and B. D. Savage, *Astrophys. J.*, 1996, **467**, 334–340.

3 S. A. Sandford, M. Nuevo, P. P. Bera and T. J. Lee, *Chem. Rev.*, 2020, DOI: DOI:10.1021/acs.chemrev.9b00560.

4 R. C. Fortenberry, T. J. Lee and J. P. Layfield, *J. Chem. Phys.*, 2017, **147**, 221101.

5 R. C. Fortenberry, C. M. Novak, J. P. Layfield, E. Matito and T. J. Lee, *J. Chem. Theor. Comput.*, 2018, **14**, 2155–2164.

6 L. Ravichandran and S. Banik, *J. Phys. Chem. A*, 2018.

7 T. J. Lee, W. D. Allen and H. F. Schaefer, III, *J. Chem. Phys.*, 1987, **87**, 7062–7075.

8 A. M. Ahern, R. L. Garrell and K. D. Jordan, *J. Phys. Chem.*, 1988, **92**, 6228–6232.

9 E. D. Simandiras, J. E. Rice, T. J. Lee, R. D. Amos and N. C. Handy, *J. Chem. Phys.*, 1988, **88**, 3187–3195.

10 J. M. L. Martin, T. J. Lee and P. R. Taylor, *J. Chem. Phys.*, 1998, **108**, 676.

11 X. Huang, E. F. Valeev and T. J. Lee, *J. Chem. Phys.*, 2010, **133**, 244108.

12 J. M. Martin, P. R. Taylor and T. J. Lee, *Chem. Phys. Lett.*, 1997, **275**, 414–422.

13 N. R. Samala and K. D. Jordan, *Chem. Phys. Lett.*, 2017, **669**, 230–232.

14 D. Moran, A. C. Simmonett, F. E. Leach III, W. D. Allen, P. v. R. Schleyer and H. F. Schaefer III, *J. Am. Chem. Soc.*, 2006, **128**, 9342–9343.

15 D. Asturiol, M. Duran and P. Salvador, *J. Chem. Theory Comput.*, 2009, **5**, 2574–2581.

16 P. B. Karadakov, *Chem. Phys. Lett.*, 2016, **646**, 190–196.

17 C. W. Bauschlicher Jr., *Chem. Phys. Lett.*, 2016, **665**, 100–104.

18 C. E. Dateo and T. J. Lee, *Spectrochim. Acta A*, 1997, **53**, 1065–1077.

19 T. J. Lee, X. Huang and C. E. Dateo, *Mol. Phys.*, 2009, **107**, 1139–1152.

20 K. Raghavachari, G. W. Trucks, J. A. Pople and E. Replogle, *Chem. Phys. Lett.*, 1989, **158**, 207–212.

21 R. C. Fortenberry and T. J. Lee, *Ann. Rep. Comput. Chem.*, 2019, **15**, 173–202.

22 X. Huang and T. J. Lee, *J. Chem. Phys.*, 2008, **129**, 044312.

23 X. Huang and T. J. Lee, *J. Chem. Phys.*, 2009, **131**, 104301.

24 X. Huang, P. R. Taylor and T. J. Lee, *J. Phys. Chem. A,* 2011, **115**, 5005–5016.

25 R. C. Fortenberry, X. Huang, J. S. Francisco, T. D. Crawford and T. J. Lee, *J. Chem. Phys.*, 2012, **136**, 234309.

26 X. Huang, R. C. Fortenberry and T. J. Lee, *Astrophys. J. Lett.*, 2013, **768**, 25.

27 D. Zhao, K. D. Doney and H. Linnartz, *Astrophys. J. Lett.*, 2014, **791**, L28.

28 R. C. Fortenberry, X. Huang, D. W. Schwenke and T. J. Lee, *Spectrochim. Acta A*, 2014, **119**, 76–83.

29 R. C. Fortenberry, T. J. Lee and H. S. P. Müller, *Molec. Astrophys.*, 2015, **1**, 13–19.

30 M. J. R. Kitchens and R. C. Fortenberry, *Chem. Phys.*, 2016, **472**, 119–127.

31 R. C. Fortenberry, *ACS Earth Space Chem.*, 2017, **1**, 60–69.

32 L. Bizzocchi, V. Lattanzi, J. Laas, S. Spezzano, B. M. Giuliano, D. Prudenzano, C. Endres, O. Sipilä and P. Caselli, *Astron. Astrophys.*, 2017, **602**, A34.

33 J. W. Huang and W. R. M. Graham, *J. Chem. Phys.*, 1990, **93**, 1583–1596.

34 W. J. Morgan, R. C. Fortenberry, H. F. Schaefer III and T. J. Lee, *Mol. Phys.*, 2019, **118**, 1.

35 D. Agbaglo, T. J. Lee, R. Thackston and R. C. Fortenberry, *Astrophys. J.*, 2019, **871**, 236.

36 E. Peeters, L. J. Allamandola, D. M. Hudgins, S. Hony and A. G. G. M. Tielens, in *Astrophysics of Dust, ASP Conference Series*, ed. A. N. Witt, G. C. Clayton and B. T. Draine, Astronomical Society of the Pacific, San Francisco, CA, 2004, vol. 309.

37 A. Tielens, *The Physics and Chemistry of the Interstellar Medium*, Cambridge University Press, Cambridge, UK, 2005.

38 A. G. G. M. Tielens, *Annu. Rev. Astron. Astrophys.*, 2008, **46**, 289–337.

39 A. M. Ricks, G. E. Douberly and M. A. Duncan, *Astrophys. J.*, 2009, **702**, 301.

40 K. A. Peterson, T. B. Adler and H.-J. Werner, *J. Chem. Phys.*, 2008, **128**, 084102.

41 J. G. Hill and K. A. Peterson, *Phys. Chem. Chem. Phys.*, 2010, **12**, 10460–10468.

42 T. H. Dunning, *J. Chem. Phys.*, 1989, **90**, 1007–1023.

43 R. A. Kendall, T. H. Dunning and R. J. Harrison, *J. Chem. Phys.*, 1992, **96**, 6796–6806.

44 D. Agbaglo and R. C. Fortenberry, *Chem. Phys. Lett.*, 2019, **734**, 136720.

45 R. C. Fortenberry, D. Peters, B. C. Ferari and C. J. Bennett, *Astrophys. J.*, 2019.

46 H.-J. Werner, P. J. Knowles, G. Knizia, F. R. Manby, M. Schütz, P. Celani, W. Györffy, D. Kats, T. Korona, R. Lindh, A. Mitrushenkov, G. Rauhut, K. R. Shamasundar, T. B. Adler, R. D. Amos, A. Bernhardsson, A. Berning, D. L. Cooper, M. J. O. Deegan, A. J. Dobbyn, F. Eckert, E. Goll, C. Hampel, A. Hesselmann, G. Hetzer, T. Hrenar, G. Jansen, C. Köppl, Y. Liu, A. W. Lloyd, R. A. Mata, A. J. May, S. J. McNicholas, W. Meyer, M. E. Mura, A. Nicklass, D. P. O'Neill, P. Palmieri, D. Peng, K. Pflüger, R. Pitzer, M. Reiher, T. Shiozaki, H. Stoll, A. J. Stone, R. Tarroni, T. Thorsteinsson and M. Wang, *MOLPRO, Version 2015.1, a Package of ab Initio Programs*, 2015, see http://www.molpro.net.

47 T. B. Adler, G. Knizia and H.-J. Werner, *J. Chem. Phys.*, 2007, **127**, 221106.

48 G. Knizia, T. B. Adler and H.-J. Werner, *J. Chem. Phys.*, 2009, **130**, 054104.

49 M. J. Frisch, G. W. Trucks, H. B. Schlegel, G. E. Scuseria, M. A. Robb, J. R. Cheeseman, G. Scalmani, V. Barone, G. A. Petersson, H. Nakatsuji, X. Li, M. Caricato, A. V. Marenich, J. Bloino, B. G. Janesko, R. Gomperts, B. Mennucci, H. P. Hratchian, J. V. Ortiz, A. F. Izmaylov, J. L. Sonnenberg, D. Williams-Young, F. Ding, F. Lipparini, F. Egidi, J. Goings, B. Peng, A. Petrone, T. Henderson, D. Ranasinghe, V. G. Zakrzewski, J. Gao, N. Rega, G. Zheng, W. Liang, M. Hada, M. Ehara, K. Toyota, R. Fukuda, J. Hasegawa, M. Ishida, T. Nakajima, Y. Honda, O. Kitao, H. Nakai, T. Vreven, K. Throssell, J. A. Montgomery, Jr., J. E. Peralta, F. Ogliaro, M. J. Bearpark, J. J. Heyd, E. N. Brothers, K. N. Kudin, V. N. Staroverov, T. A. Keith, R. Kobayashi, J. Normand, K. Raghavachari, A. P. Rendell, J. C. Burant, S. S. Iyengar, J. Tomasi, M. Cossi, J. M. Millam, M. Klene, C. Adamo, R. Cammi, J. W. Ochterski, R. L. Martin, K. Morokuma, O. Farkas, J. B. Foresman and D. J. Fox, *Gaussian~16 Revision C.01*, 2016, Gaussian Inc. Wallingford CT.

50 C. Møller and M. S. Plesset, *Phys. Rev.*, 1934, **46**, 618–622.

51 Q. Yu, J. M. Bowman, R. C. Fortenberry, J. S. Mancini, T. J. Lee, T. D. Crawford, W. Klemperer and J. S. Francisco, *J. Phys. Chem. A*, 2015, **119**, 11623–11631.

52 B. Finney, R. C. Fortenberry, J. S. Francisco and K. A. Peterson, *J. Chem. Phys.*, 2016, **145**, 124311.

53 W. D. Allen and coworkers, 2005, *INTDER* 2005 is a General Program Written by W. D. Allen and Coworkers, which Performs Vibrational Analysis and Higher-Order Non-Linear Transformations.

54 I. M. Mills, in *Molecular Spectroscopy - Modern Research*, ed. K. N. Rao and C. W. Mathews, Academic Press, New York, 1972, pp. 115–140.

55 J. K. G. Watson, in *Vibrational Spectra and Structure*, ed. J. R. During, Elsevier, Amsterdam, 1977, pp. 1–89.

56 D. Papousek and M. R. Aliev, *Molecular Vibration-Rotation Spectra*, Elsevier, Amsterdam, 1982.

57 J. F. Gaw, A. Willets, W. H. Green and N. C. Handy, 1996, *SPECTRO program*, version 3.0.

58 J. M. L. Martin, T. J. Lee, P. R. Taylor and J.-P. François, *J. Chem. Phys.*, 1995, **103**, 2589–2602.

59 J. M. L. Martin and P. R. Taylor, *Spectrochim. Acta A*, 1997, **53**, 1039–1050.

60 R. C. Fortenberry, X. Huang, J. S. Francisco, T. D. Crawford and T. J. Lee, *J. Chem. Phys.*, 2011, **135**, 134301.

61 R. C. Fortenberry, X. Huang, J. S. Francisco, T. D. Crawford and T. J. Lee, *J. Chem. Phys.*, 2011, **135**, 214303.

62 R. C. Fortenberry, X. Huang, J. S. Francisco, T. D. Crawford and T. J. Lee, *J. Phys. Chem. A.*, 2012, **116**, 9582–9590.

63 X. Huang, R. C. Fortenberry and T. J. Lee, *J. Chem. Phys.*, 2013, **139**, 084313.

64 R. C. Fortenberry, X. Huang, T. D. Crawford and T. J. Lee, *J. Phys. Chem. A*, 2014, **118**, 7034–7043.

65 W. J. Morgan and R. C. Fortenberry, *Spectrochim. Acta A*, 2015, **135**, 965–972.

66 W. J. Morgan and R. C. Fortenberry, *J. Phys. Chem. A*, 2015, **119**, 7013–7025.

67 R. A. Theis and R. C. Fortenberry, *J. Phys. Chem. A*, 2015, **119**, 4915–4922.

68 D. Agbaglo and R. C. Fortenberry, *Int. J. Quantum Chem.*, 2019, **119**, e25899.

Two vibrational frequencies for this molecule correlate with observed but unknown interstellar infrared emission features.